Soft Matter

Pulling simulation predicts mixing free energy for binary mixtures

Journal:	*Soft Matter*
Manuscript ID	SM-ART-08-2022-001065.R1
Article Type:	Paper
Date Submitted by the Author:	29-Sep-2022
Complete List of Authors:	Mkandawire, Wezi; The Pennsylvania State University University Park Milner, Scott; The Pennsylvania State University University Park

Journal Name

ARTICLE TYPE

Cite this: DOI: 00.0000/xxxxxxxxxx

Pulling simulation predicts mixing free energy for binary mixtures

Wezi D. Mkandawire and Scott T. Milner

Received Date
Accepted Date

DOI: 00.0000/xxxxxxxxxx

Predicting the mixing free energy of mixing for binary mixtures using simulations is challenging. We present a novel molecular dynamics (MD) simulation method to extract the chemical potential $\mu(X)$ for mixtures of species A and B. Each molecule of species A and B is placed in equal and opposite harmonic potentials $\pm(1/2)U_{ex}(x)$ centered at the middle of the simulation box, resulting in a nonuniform mole fraction profile $X(z)$ in which A is concentrated at the center, and B at the periphery. Combining these, we obtain $U_{ex}(X)$, the exchange chemical potential required to induce a given deviation of the mole fraction from its average. Simulation results for $U_{ex}(X)$ can be fitted to simple free energy models to extract the interaction parameter χ for binary mixtures. To illustrate our method, we investigate benzene-pyridine mixtures, which provide a good example of regular solution behavior, using both TraPPE united-atom and OPLS all-atom potentials, both of which have been validated for pure fluid properties. χ values obtained with the new method are consistent with values from other recent simulation methods. However, the TraPPE-UA results differ substantially from the χ obtained from VLE experimental data, while the OPLS-AA results are in reasonable agreement with experiment, highlighting the importance of accurate potentials in correctly representing mixture behavior.

1 Introduction

Predicting the mixing free energy of binary mixtures enables the prediction of phase behavior, which is a fundamental task and challenge for physical chemists and chemical engineers. Within the context of regular solution theory, non-ideal contributions to the mixing free energy are often quantified by an effective interaction parameter χ. Intuitively, χ represents the cost of placing two unlike species in a mixture next to each other, reflecting net unfavorable interactions between them.[1] As χ increases, the species have an increased propensity to demix.

Intuitively, we expect local interactions between species in a mixture to depend sensitively on chemical details, so atomistic simulations would appear to be well suited for investigating mixing free energies. However, molecular dynamics (MD) simulations only give direct access to quantities that depend on coordinates, so that measuring the entropy or free energy requires special techniques.

Many attempts have been made to calculate mixing free energies. One approach determines the mixing free energy from the difference in the thermodynamic work to take a species from vacuum into pure and mixed systems.[2,3,4] However, it takes a very large amount of work to remove a molecule from solution into vacuum, so values computed in this way inevitably involve subtraction of two large values to obtain a small result, with consequent large uncertainties. Versions of this approach that measure chemical potential by attempting to insert molecules into dense fluids also face challenges of poor statistics, because the chemical potential depends exponentially on the extremely low probability of successful insertion.

Perego et al. have recently improved upon the insertion method, using metadynamics to enhance concentration fluctuations to increase the extremely low success rate for insertion, for a Lennard-Jones fluid.[5] However, this approach will be increasingly challenging for atomistic simulations of larger molecules, for which the bare insertion probabilities are progressively smaller.

Another commonly used approach to obtain chemical potentials is provided by the Kirkwood-Buff equations,[6] which relate derivatives of chemical potentials with respect to concentrations to volume integrals of pair correlation functions (Kirkwood-Buff integrals). However, this approach is challenging, in that 1) very large simulation systems are required to obtain the pair correlation functions out to large distances such that the KB integrals converge; and 2) multiple simulations at different concentrations plus numerical integrations are required to obtain chemical potentials versus concentration, which then can be integrated once more to obtain excess free energies.[7–9]

Quite recently, Heidari et al. developed a sophisticated method for measuring excess chemical potentials from atomistic simulation.[10] The method describes molecules with atomistic interactions in a subregion, and as ideal gas elsewhere, with a position-

Pennsylvania State University, University Park, Pennsylvania, USA

† Electronic Supplementary Information (ESI) available: [details of any supplementary information available should be included here]. See DOI: 00.0000/00000000.

dependent crossover between Hamiltonians. Molecules equilibrate by diffusing across the system; single-molecule external potentials are applied in the ideal gas region, and adjusted to enforce constant density across the system. The potentials then have the interpretation of excess chemical potential. This method avoids thermodynamic integration, but requires elaborate custom coding not available in standard simulation platforms, and provides the chemical potential at only one value of concentration per simulation.

In our group, we have recently developed methods using "morphing" simulations to get the mixing free energy.[11 12 13 14] In this approach, one species in a mixture is transformed or"morphed" into another species, by progressively varying force field parameters. A parameter λ quantifies the progress along the morphing path. By integrating the change in average energy with respect to λ, the thermodynamic work is calculated to morph one species into another. From the difference between the thermodynamic work to morph one species to another in a mixed system versus a pure system, the excess mixing free energy can be computed. This approach works well for idealized bead-spring model blends; however, it is limited in its application to atomistic simulations of real molecules, because of the difficulty in morphing between structurally dissimilar molecules.

In another recent approach, which we call "mutual ghosting", the thermodynamic work to separate species A and B in a mixture can be computed by progressively weakening the A-B attractions to induce phase separation. and integrating the change in system energy along the path.[15] Once phase separation is induced between the two species, the interfacial tension between the coexisting pure phases is measured by standard techniques. The mixing free energy is then the work to induce the phase-separated state, minus the free energy of the resulting interface.

This method does not require species to be structurally similar. However, it is somewhat involved; multiple simulations are required to morph the system to the phase separated state, and accurately simulating the interfacial tension between the separated species can require long equilibration. Finally, the method computes the entire mixing free energy (including the ideal-gas contribution), not just the excess. So for near-ideal systems such as miscible polymer blends, measuring the mixing free energy accurately enough to infer the χ parameter can be challenging.

In this work, we develop a new simulation method to calculate the mixing free energy versus concentration for A-B binary mixtures. Equal and opposite harmonic potentials $\pm U(z)$ centered at the middle of the simulation box are applied to every molecule of the two species, so that one species is pulled towards the center while the other is pushed towards the periphery, inducing a nonuniform mole fraction profile $X(z)$. (We emphasize that the potentials must be applied to *every molecule individually*, not simply to the center of mass of each species.)

Figure 1 shows a snapshot (made using VMD[16]) of such a simulation for an equimolar mixture of benzene and pyridine, in which the pyridine molecules are each pulled towards the center (in the horizontal direction in the image) and the benzene pushed towards the boundaries.

In essence, we are imposing an external contribution $U_{ex}(z) = 2U(z)$ to the exchange chemical potential. The system responds by rearranging the molecules, such that the local chemical potential versus mole fraction cancels the imposed external potential, and restores equilibrium throughout the system. By combining the imposed exchange potential $U_{ex}(z)$ with the measured mole fraction $X(z)$ we obtain $U_{ex}(X)$, the external potential required to shift the mole fraction to X from its average value. In this way, we effectively measure the exchange chemical potential versus mole fraction. Numerically integrating this exchange chemical potential would give the mixing free energy, without assuming any particular model.

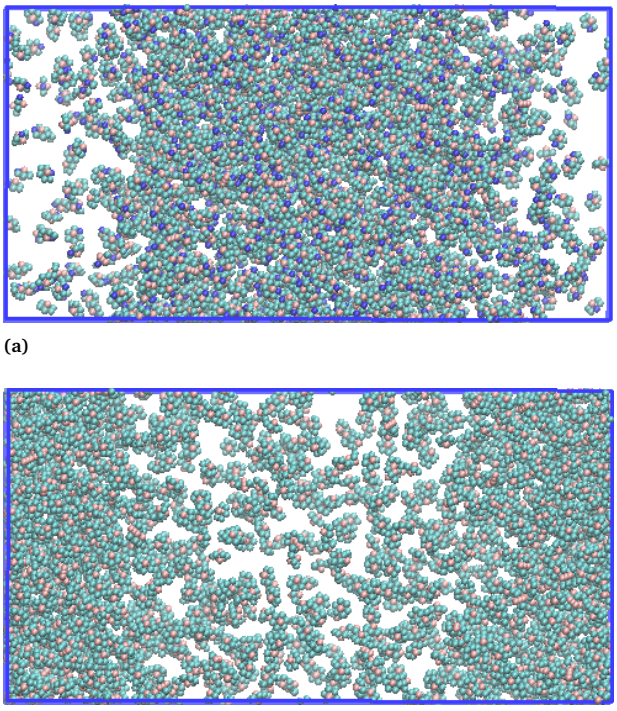

(a)

(b)

Fig. 1 Equimolar benzene-pyridine mixture, in which pyridine (shown in a) is pulled towards the center, and benzene (shown in b) is pushed towards the periphery.

Our approach is related in spirit to work of Mehrotra et al., who applied a constant gravitational field in a Monte Carlo simulation of a Lennard-Jones liquid.[17] The linear gravitational potential induces a nonuniform concentration profile, which shifts the local chemical potential to cancel the applied field, from which the chemical potential versus concentration can be inferred. This approach could in principle be generalized to a two-component mixture, by applying a constant gravitational field to only one component. However, this would only work in a system with a bottom wall, which would induce undesirable surface ordering artifacts, particularly for linear or plate-like molecules, such as oligomers, polymers, or polyaromatics.

In this paper, to interpret the results of our molecular pulling simulations, we compare the resulting behavior of $U_{ex}(X)$ to predictions of a model free energy function. For regular solutions of small molecules, the natural choice is a Margules model, in which non-ideal mixing effects are parameterized in terms of bi-

nary interactions between mole fractions. For a binary mixture, this model contains a single χ parameter, which can be fit to the observed $U_{ex}(X)$ behavior. If the resulting fit is uniformly good throughout the range of mole fractions explored, the choice of model is phenomenologically justified *a posteriori*.

More generally, fitting the excess free energy of a binary mixture may require an interaction parameter $\chi(X)$ that depends on mole fraction in some arbitrary fashion. Because our method can determine $U_{ex}(X)$ over a wide range of mole fractions with a single simulation, it is well adapted to test for mole-fraction dependence of χ, and to fit such dependence when necessary.

The status of χ parameter values so obtained is analogous to values from neutron scattering experiments on polymer blends fitted to the random-phase approximation (RPA), which describes concentration fluctuations in miscible blends. Indeed, our method may be regarded as the response function analog of such measurements; instead of observing thermally driven concentration fluctuations, we apply an external potential to induce a concentration response. In simulations, this method is more convenient than watching fluctuations, because we control the shape of the external potential, and measure the time-averaged response over a long simulation for improved signal-to-noise.

To illustrate our new method, we investigate an equimolar mixture of benzene and pyridine, which serves as a good example of regular solutions, since the molecules roughly the same size and shape.[18] The large dipole of pyridine (2.26 Debye) leads to significant non-ideal mixing, as pyridine dipoles interact with each other, but not with nonpolar benzene. Moreover, vapor-liquid equilibrium (VLE) data for benzene and pyridine mixtures is available,[19] from which an experimental χ parameter can be calculated, by fitting model free energy predictions of vapor pressure and vapor-phase composition to experiment.

2 Mixing free energy

For mixtures of molecules of similar size and shape like benzene and pyridine, the mixing free energy is reasonably modeled by regular solution theory:

$$\beta\Delta G = \sum_i X_i \log X_i + \sum_{ij} \chi_{ij} X_i X_j + \beta \sum_i X_i U_i \tag{1}$$

In Eqn. 1, the first term represents ideal mixing, the second models non-ideal contributions in terms of binary interactions between constituent mole fractions, and the final term includes the effect of external potentials we apply to the different species. For a truly ideal solution, in which the two species are physically identical and only distinguished by labels, the second terms vanish (ideal solutions are experimentally well approximated by mixtures of deuterated and non-deuterated species).

In writing Eqn. 1, we have neglected any square-gradient contributions to the local free energy. Of course, we are applying potentials $U(z)$ to our simulation that vary substantially over distances of 10 nm or so. As described in detail below, we take pains both to minimize gradient effects, and to check that gradient contributions to the local chemical potential are small. Briefly, we use an oblong simulation box, twice as long in the z direction along which $U(z)$ varies as in the transverse dimensions. Next, we check that simulations performed in longer and shorter boxes give consistent results for the concentration profile when harmonic potentials of the same amplitude are applied in each case.

Finally, we check that simulations applied to truly ideal mixtures (labeled and unlabeled benzene) are consistent with predictions of ideal solution theory (i.e., Eqn. 1 with $\chi = 0$) and no gradient terms. We expect square-gradient contributions to the chemical potential even in ideal mixtures, with a characteristic length scale of the molecule itself. These reflect the increased thermodynamic cost of spatially rapid variations in the concentration, even of physically identical species.

To predict the nonuniform concentration profile resulting from application of potentials $U_i(z)$ to component i, we minimize the Gibbs free energy subject to the constraint that the mole fractions sum to unity ($\sum_i X_i = 1$), using the method of Lagrange multipliers. Minimization with respect to X_1 and X_2 leads to

$$\begin{aligned} 0 &= \log X_1 + \chi X_2 + \beta U_1 - \alpha \\ 0 &= \log X_2 + \chi X_1 + \beta U_2 - \alpha \end{aligned} \tag{2}$$

in which α is the Lagrange multiplier conjugate to the sum of the mole fractions.

Corresponding to our simulations in which we pull on the two species with equal and opposite harmonic potentials, we write $U_1 = U$ and $U_2 = -U$, and take $X_1 = X$ and $X_2 = 1 - X$; subtracting the two equations gives

$$-\beta U_{ex}(X) = \log\left(\frac{X}{1-X}\right) + \chi(1-2X) \tag{3}$$

Here $U_{ex}(z) = 2U(z)$ is the exchange potential, i.e., the energy change on transforming the species of a molecule at z. Eqn. 3 predicts the shape of $U_{ex}(X)$, with χ as an adjustable parameter.

This result evidently respects the symmetry of the regular solution free energy model, with respect to interchange of the two species. In Eqn. 3, the result is unchanged if we exchange X with $1-X$ and $U_{ex}(X)$ with $-U_{ex}(X)$; physically, this corresponds to exchanging the labels on the two species.

3 Simulation setup

In our investigations, we simulate two different systems: pure benzene, and an equimolar mixture of benzene and pyridine, both at 300K. Each system consists of 3072 molecules in a 6 x 6 x 12 nm box with periodic boundary conditions in all directions. The box is twice as long in the z-direction along which the potential $U(z)$ varies, to minimize the effect of gradient terms on the local chemical potential, which we neglect in our analysis of the simulation results. (Below, we describe how we validate this approximation.)

Our simulations are run in Gromacs, using the TraPPE united atom potentials for benzene and pyridine, which have been validated against pure fluid properties.[20–22] The TraPPE potentials represent benzene and pyridine by six united atoms (CH or N), plus three additional charge-bearing "virtual sites" near the center of the rings to account for the electrostatic quadrupole of the π orbitals. Hence 3072 molecules total 27,648 atoms.

The simulations were executed on 16 cores with support from

1 GPU (half of an NVidia K80), with a 2 fs timestep, 1.4nm cutoffs for Lennard-Jones interactions, and particle-mesh Ewald evaluation of Coulomb interactions. The simulations run at 80 ns/day when no potentials are applied, and at 35 ns/day with harmonic potentials acting on all the molecules.

Each system is equilibrated for 4 ns with semi-isotropic pressure control, such that the simulation box can adjust its transverse dimensions but not its length along the z direction, along which the external potentials $\pm U(z)$ vary. We keep the box dimension along z fixed so that potentials with the same center and spring constant can be applied to all systems. The transverse dimensions adjust slightly, from the initially constructed 6nm down to about 5.94 nm.

From the mean-square displacement versus time, the diffusion constant of each species was measured as 2.6 ^{2}/ns for benzene and 2.5 nm^2/ns for pyridine. The 4 ns equilibration time is sufficient for molecules to diffuse across the entire system. After equilibration, composition profile data was collected for 200 ns. As a further check on equilibration, we verify that the density profile for each species from the first and last half of the run are the same.

To explore ideal and regular solution behavior, we perform three different pulling simulations. For pure benzene, we pull half the molecules towards the center, and push the other half away. This serves as a model ideal solution. For the equimolar benzene-pyridine mixture we perform two simulations, in which we a) pull benzene towards the center and push pyridine away, and b) pull pyridine towards the center and push benzene away. Although they lead to different mole fraction profiles $X(z)$, these two simulations should be physically equivalent in the resulting profile $U_{ex}(X)$, and thus serve as an additional check on our method.

Figure 2 displays results for the time-averaged mole fraction profiles $X(z)$ for all three pulling simulations, as well as the total number density profiles for each case. (The coordinate $z = 0$ is the left side of the box, and $z = 6$ is the box center; the left and right halves of the profiles have been averaged, and the figure displays the resulting average.)

The mole fraction profiles are evidently smooth and free of noise, indicating good statistics. The total number density profiles are nearly flat, indicating that the potentials we have applied are not so strong as to have significantly altered the liquid density.

In Fig. 2, the range of mole fractions produced by the applied potential is substantial, ranging from about 0.15–0.75 for the ideal solution of benzene in benzene, and from about 0.1–0.8 for the benzene-pyridine mixture. The spread of X values determines the range over which we measure the chemical potential and test the model free energy predictions.

The spread of X is governed by our choice of amplitude for the harmonic potential $U_{ex}(z)$. By trial and error, we chose the potential applied to every molecule of each species $U_{A,B}(z) = \pm\frac{1}{2}Kz^2$ such that the energy difference between the middle and boundary of the box is $\frac{3}{2}kT$. For a box of length 12 nm in the z-direction, this gives a spring constant $K = 0.2078$ kJ/(mol nm^2). Correspondingly, the exchange potential $U_{ex}(z)$ varies by 3kT from the middle to the boundary of the box.

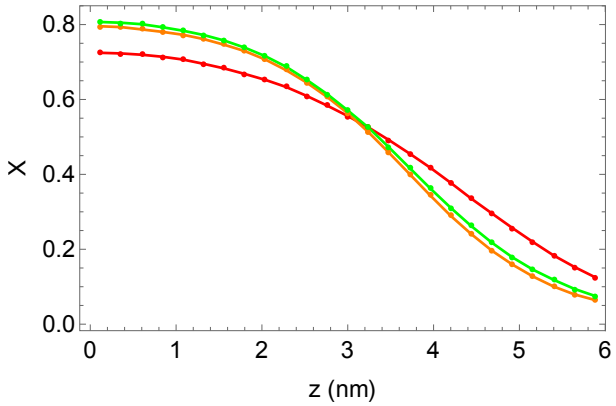

Fig. 2 Pulled species mole fraction X vs. box coordinate (nm); pulled species is benzene in pure benzene (red), benzene in mixture (green), and pyridine in mixture (orange).

To apply harmonic potentials to each and every molecule in the system, we make use of shell scripts to write the necessary pull code options for each molecule to the `.mdp` (Gromacs MD parameter) file. They are repetitive, differing only in their indices, so well adapted to a simple script in which an index variable in a "template" file is replaced using the Unix utility `sed`. Likewise, we must include index groups for each molecule in the system `.ndx` (Gromacs index) file, again generated with a brief shell script.

4 Results

Qualitatively, Fig. 2 shows the expected behavior of regular versus ideal solutions; for the same strength potentials $U_{ex}(z)$, the regular solution results (yellow and green), with net repulsive interactions between species, exhibits a stronger response of the mole fraction $X(z)$ as compared to the ideal solution (red), with no repulsive interactions.

The mole fraction profiles $X(z)$ for pulling benzene from the mixture (green) and pulling pyridine from the mixture (yellow) are very similar, which is consistent with a simple regular solution model in which the two species are symmetric under interchange.

To proceed further with our analysis, we combine the measured mole fraction profiles $X(z)$ with the imposed exchange potential $U_{ex}(z)$, to determine the imposed potential versus mole fraction $U_{ex}(X)$, shown in Fig. 3 for all three cases.

(Note that in Fig. 3, we have slightly shifted the applied potential so that $U = 0$ at $X = 1/2$, consistent with the symmetry of the regular solution model under interchange of species for an equimolar mixture.)

Consistent with our remarks on the concentration profile in Fig. 2, Fig. 3 shows that a weaker potential suffices to induce a given degree of separation in the benzene-pyridine mixture as compared to pure benzene. Repulsive interactions in the regular solution confer a tendency to demix, and amplify the response to the external potential.

In the pure benzene system, a given benzene molecule sees no difference between a "pulled" benzene and a "pushed" benzene, so its placement in the simulation box is simply determined by its Boltzmann factor in the potential $U(z)$. Whereas in the mixture, pyridine molecules prefer to be with other pyridines, and

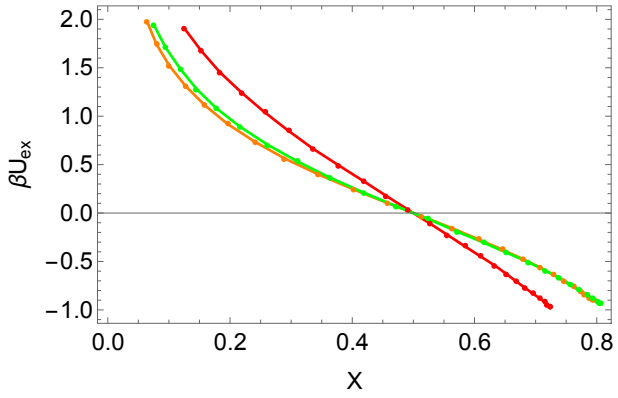

Fig. 3 Imposed exchange potential U_{ex} vs. mole fraction X for benzene pulled from benzene (red), pyridine pulled from mixture (orange), and benzene pulled from mixture (green).

benzenes with other benzenes; a given pyridine molecule in the mixture feels the pull from the potential $U(z)$, as well as an extra "pull" towards other pyridines likewise gathered towards the potential minimum.

For the ideal mixture of labeled and unlabeled benzene, the results for $U_{ex}(X)$ are well described by Eqn. 3 with $\chi = 0$ appropriate for an ideal solution, as shown in Fig. 4. The good agreement

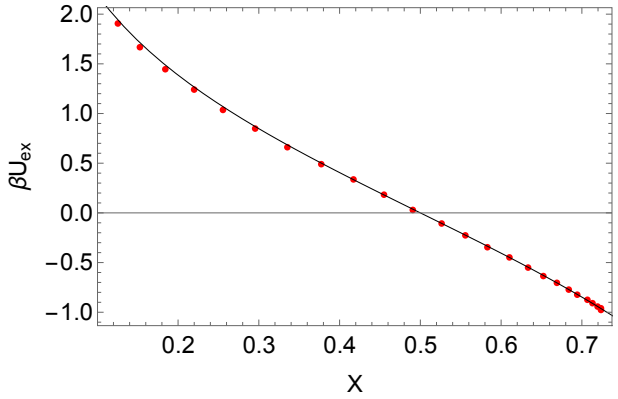

Fig. 4 Ideal $U_{ex}(X)$ data (points) compared to $U_{ex}(X)$ prediction for ideal solution (curve).

of the ideal solution theory without contributions from gradient terms supports our assumption that with this size simulation box, gradient terms can be neglected.

The regular solution model we want to use to analyze our simulation results is symmetric under interchange of species. This should be a reasonable approximation for benzene and pyridine, since they have roughly the same shape and size. We can check whether the simulation results respect that symmetry, by plotting $U_{ex}(X)$ for a given pulling simulation together with $-U_{ex}(1-X)$, which corresponds to exchanging X with $1-X$ and U_{ex} with $-U_{ex}$, as results from exchanging the roles of the two species.

Fig. 5 shows the results of this comparison, for a) the data in which pyridine is pulled to the center from the mixture, and b) the data in which benzene is pulled to the center. In both cases, the anticipated symmetry is well respected, with tolerably small deviations.

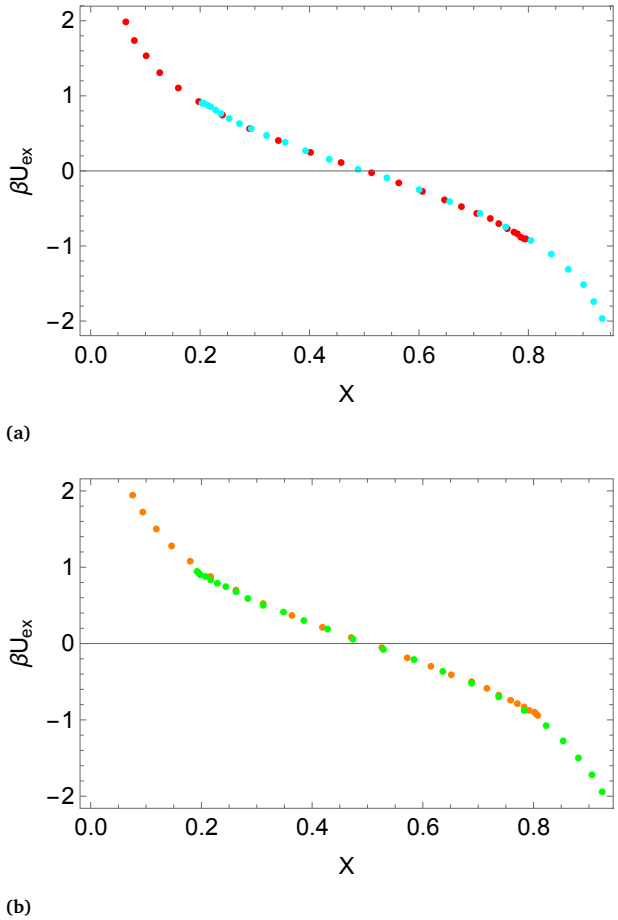

Fig. 5 (a) Original (red) and "exchanged" (blue) $U_{ex}(X)$ for pyridine pulled to the center, and (b) original (orange) and "exchanged" (green) $U_{ex}(X)$ for benzene pulled to the center, in benzene-pyridine mixtures.

In similar fashion, we can compare the $U_{ex}(X)$ results for the two different simulations, in which pyridine or benzene was pulled to the center of the mixture. If the solution is regular, then $U_{ex}(X)$ for the case in which pyridine is pulled towards the center should overlay with $-U_{ex}(1-X)$ for the case in which benzene is pulled towards the center. Fig. 6 makes this comparison, which again shows our results for benzene-pyridine mixtures are consistent with this exchange symmetry.

Finally, we fit a value for χ to the data from both pulling simulations on the benzene-pyridine mixture, symmetrized with respect to species exchange, both within and between the two data sets. A linear least-squares fit gives $\chi = 0.763 \pm 0.005$. Fig. 7 displays the combined $U_{ex}(X)$ results versus the regular solution theory prediction, which evidently gives a very good fit across the entire range of mole fractions explored, lending support to our choice of the simple free energy model for this regular solution.

The good fit of regular solution theory to simulation results throughout the entire mole fraction range is strong evidence that for this system, a constant χ parameter suffices. More generally, $\chi(X)$ may be taken to depend on mole fraction X; indeed, a free energy curve of any shape whatsoever can be described phenomenologically by such a function.

If the predicted curve $U_{ex}(X)$ with constant χ fit well near

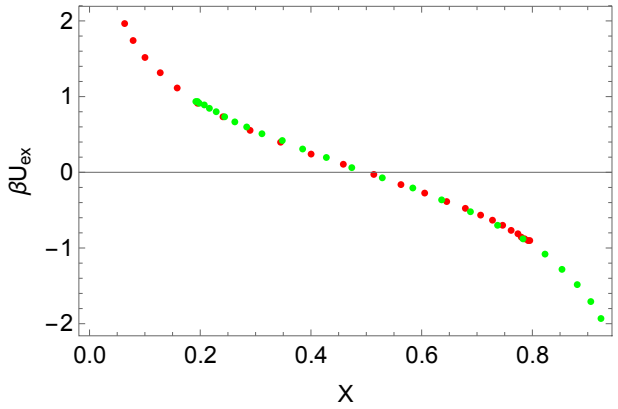

Fig. 6 Original pyridine-pulling (red) and "exchanged" benzene-pulling (green) $U_{ex}(X)$ data.

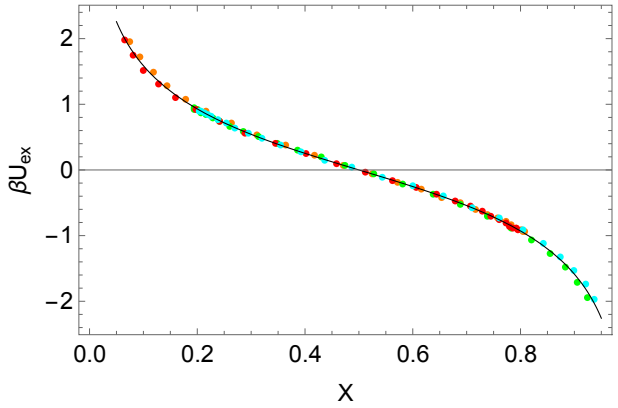

Fig. 7 Combined and symmetrized pyridine and benzene $U_{ex}(X)$ data versus regular solution $U_{ex}(X)$ with $\chi = 0.763$.

$X + 1/2$ but deviated at the ends of the range, it would suggest some $\chi(X)$ would be needed to describe the data. Qualitatively, if $U_{ex}(X)$ with constant χ underpredicted the deviation of X from $1/2$ on one end of the data, it would imply χ was larger at that end of the data than near $X = 1/2$, and so forth. One can envision deviations corresponding to positive or negative linear or quadratic dependence of $\chi(X)$ on $X - 1/2$, all of which are phenomenologically found for example in various polymeric systems. The derivation of Eqn. 3 could be extended to include terms resulting from the derivative of $\chi(X)$. Here at least, such refinements are unnecessary.

4.1 Comparison to simulation and experiment

The interaction parameter χ for benzene and pyridine has been determined experimentally, as well as in recent "mutual ghosting" simulations, which were performed using the same TraPPE potentials as used in the present work. The χ value obtained by mutual ghosting simulations is 0.79,[15] reassuringly close to the value obtained here by our pulling approach.

We obtain an experimentally derived value for χ from vapor-liquid equilibrium (VLE) data, by comparing the vapor pressure and vapor mole fraction as a function of liquid mole fraction to regular solution model predictions, and adjusting χ for the best fit. Fig. 8 displays for benzene-pyridine mixtures the vapor-liquid equilibrium pressure P and vapor mole fraction data y versus pyridine liquid mole fraction X.[19]

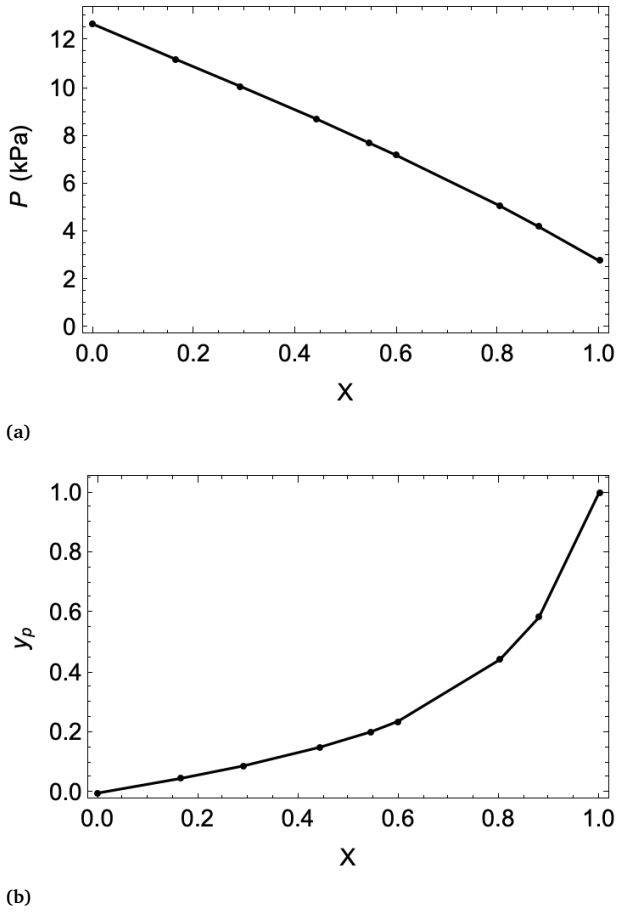

Fig. 8 (a) Vapor pressure P (kPa) vs. pyridine liquid mole fraction X; (b) pyridine vapor mole fraction y_p vs. pyridine liquid mole fraction X.

To predict the VLE behavior, we start by writing the gas and liquid chemical potentials for species i as

$$\mu_i^g = \mu_i^* + kT\log(\frac{P_i}{P_o})$$
$$\mu_i^l = \mu_i^{pure} + \Delta\mu_i^{excess} \quad (4)$$

For the gas (assumed ideal), μ_i^* is the standard chemical potential, P_i is the partial pressure of component i, and P_o is the reference pressure of the system. For the liquid, μ_i^{pure} is the chemical potential of a pure liquid of species i, and $\Delta\mu_i^{excess}$ is the excess chemical potential.

At vapor-liquid equilibrium the liquid and gas phase chemical potentials are equal, $\mu_i^g = \mu_i^l$. We can simplify the equations by introducing the vapor pressure P_i^{sat} of pure component i. For pure fluids, we have

$$\mu_i^{pure} = \mu_i^* + kT\log(\frac{P_i^{sat}}{P_o}) \quad (5)$$

which relation can be used to eliminate $\mu_i^{pure} - \mu_i^*$ in terms of P_i^{sat},

leading to

$$\Delta\mu_i^{excess} = kT\log(\frac{P_i}{P_i^{sat}}) \tag{6}$$

Equation 1 is the free energy per particle G/N. Differentiating with respect to the number of particles N_i of component i gives the excess chemical potential in terms of the interaction parameter χ and liquid mole fraction X. With subscripts p and b denoting pyridine and benzene, we find $\Delta\mu_p^{excess}$ and $\Delta\mu_b^{excess}$ from the excess free energy per particle $G(N_p,N_b)$:

$$\begin{aligned}\Delta\mu_p^{excess} &= kT\log(X)+\chi(1-X)^2\\ \Delta\mu_b^{excess} &= kT\log(1-X)+\chi X^2\end{aligned} \tag{7}$$

Combining Eqns. 6 and 7, we obtain the vapor pressure $P(X)$ as a function of pyridine liquid mole fraction X:

$$P(X) = P_p^{sat}Xe^{\chi(1-X)^2}+P_b^{sat}(1-X)e^{\chi X^2} \tag{8}$$

In Eqn. 8, the two terms correspond to the pyridine and benzene partial pressures $P_p(X)$ and $P_b(X)$. Because we regard the vapor as an ideal gas, the vapor mole fraction of pyridine $y_p(X)$ equals the ratio of the pyridine partial pressure to the total pressure:

$$y_p(X) = \frac{P_p(X)}{P(X)} \tag{9}$$

Eqs. 8 and 9 can be fit to the experimental $P(X)$ and $y_p(X)$ data to find an experimental value of χ. To carry out the comparison and fit of theory to the data, it is useful to focus on the ratio between the pressure and vapor mole fraction and their ideal-solution limits, as shown in Fig. 9.

The colored curves in Fig. 9 are predictions for different values of $\chi = 0, 0.05, 0.1, 0.15, 0.2$ (respectively red, orange, yellow, green, blue). Qualitatively, a repulsive interaction between the two species boosts the vapor pressure, particularly for intermediate mixtures. Evidently, the VLE data is rather sensitive to χ, and thus a good way to determine its value.

To determine experimental χ, we fit simultaneously the vapor pressure and composition data, both represented as ratios with respect to the ideal-solution limit. Since the values in Figs. 9 a) and b) have appreciably different ranges, minimizing the sum of square errors for the two sets of ratios would fit the vapor mole fraction ratio data with its wider range of values at the expense of the pressure ratio data.

To remedy this, we scale the vapor mole fraction ratio data such that it has a range comparable to the pressure ratio data. We achieve this by multiplying each vapor mole fraction ratio value by the ratio of the standard deviations σ_P and σ_{y_p} of the pressure ratio data and vapor mole fraction ratio data respectively. Having thus rescaled the data sets so that errors in fitting them are rendered equally important, we minimize the combined square error for the two data sets with respect to the prediction.

Figs. 9 a) and b) displays the resulting fit (dashed lines), corresponding to an interaction parameter of $\chi = 0.210 \pm 0.004$. This value evidently does not agree with the values obtained by two different simulation approaches. The simulation methods both use the TraPPE potentials, and give consistent results. This suggests both methods are working properly, and that the discrepancy between simulation and experiment reflects systematic errors in the TraPPE potentials, which were validated for pure fluids but not for mixture behavior.

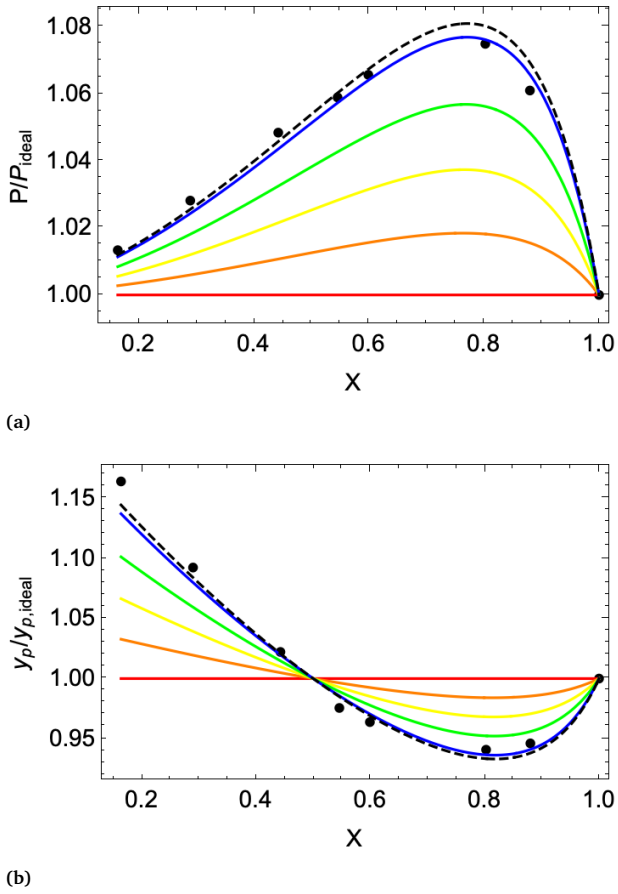

Fig. 9 (a) Pressure ratio vs. pyridine liquid mole fraction X data (black) and (b) pyridine vapor mole fraction ratio vs. pyrdine liquid mole fraction X data (black) with models where $\chi = 0$ (red), 0.05 (orange), 0.1 (yellow), 0.15 (green), 0.2 (blue), and 0.21 (purple).

5 All-atom potential results

To explore the sensitivity of results for χ to the choice of force fields, we repeated the pulling simulations for the benzene-pyridine mixture using another well-validated and widely used potential, the OPLS-AA (Optimized Potential for Liquid Simulations) all-atom potential.[23–25] Like TraPPE-UA, the OPLS-AA potentials have been validated for a wide range of organic liquids, by comparing predictions for liquid physical properties to measured values. (A useful source of such comparisons is the compendium at `virtualchemistry.org`.)

In this second set of simulations, we use the same number of molecules and system dimensions; the same timestep, temperature, cutoff, and harmonic potential strengths; the same equilibration procedure and run lengths; in short, everything is the same except the force field. The all-atom system has slightly more atoms (35238 versus 27648), and a slightly different density than the UA system (the transverse dimension grows to 6.044Å, rather than shrinking to 5.938Å). The simulations run at compa-

rable rates on the same hardware (60 ns/day all-atom versus 80 ns/day UA without harmonic potentials, and comparable rates of 35 ns/day with potentials applied).

Just because OPLS is an all-atom potential in which hydrogens are explicitly represented, while TraPPE is a united atom potential in which hydrogens are lumped together with the atom to which they are bonded, does not mean OPLS necessarily provides a more accurate representation of real molecules than TraPPE. A united-atom potential can be tuned to faithfully represent real molecules, and an all-atom potential can be improperly parameterized and fail miserably.

However, in the present case, it appears that OPLS does much better than TraPPE in representing the mixture behavior of benzene and pyridine. This is evident qualitatively in Fig. 10, which (compared to Fig. 3 for TraPPE) shows a much smaller deviation of the pulling results for $U_{ex}(X)$ for benzene pulled from pyridine (green) and vice versa (orange) compared to the ideal case of benzene pulled from benzene (red).

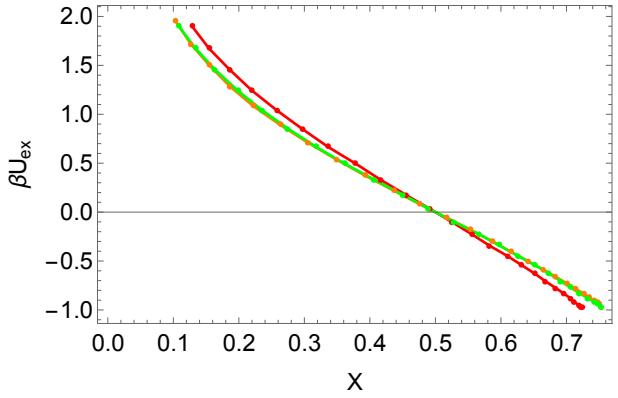

Fig. 10 Imposed exchange potential U_{ex} vs. mole fraction X for benzene pulled from benzene (red), pyridine pulled from mixture (orange), and benzene pulled from mixture (green), for simulations using OPLS-AA potentials.

As for the united-atom pulling results, the all-atom pulling results respect the exchange symmetries expected for a regular solution. Likewise, a concentration-independent χ parameter equal to 0.282 ± 0.002 gives an excellent fit to the pulling results, as shown in Fig. 11 (compare Fig. 7 for TraPPE results).

Although not perfect, the pulling value using OPLS potentials is much closer to the experimental result (see Table **??**) highlighting the importance of well-adjusted forcefields that faithfully represent real molecules in simulations of fluid mixtures.

Source	χ
TraPPE-UA	0.763 ± 0.005
OPLS-AA	0.282 ± 0.002
VLE fit	0.210 ± 0.004

Table 1 Results for benzene-pyridine χ from pulling simulations using TraPPE-UA potentials, OPLS-AA potentials, and from fitting to vapor-liquid equilibrium data.

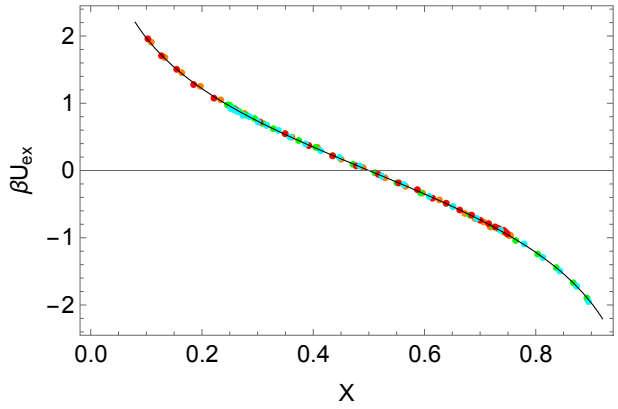

Fig. 11 Combined and symmetrized pyridine and benzene $U_{ex}(X)$ data versus regular solution $U_{ex}(X)$ with $\chi = 0.282 \pm 0.002$, obtained by fitting all-atom results.

6 Conclusion

We have presented a new "pulling" method to predict the mixing free energy of binary mixtures using molecular dynamics (MD) simulations. The method works by applying equal and opposite harmonic potentials $U(z)$ to every molecule of both species, to induce a nonuniform mole fraction $X(z)$ in the system. In essence, the externally applied potentials shift the local exchange chemical potential; the system responds by adjusting the local concentrations until equilibrium is restored.

By combining the observed mole fraction profile $X(z)$ with the imposed exchange potential $U_{ex}(z)$, we can determine the potential $U_{ex}(X)$ required to shift the mole fraction to a given degree. The interaction parameter χ for a binary mixture can be determined by comparing predictions of regular solution theory for $U_{ex}(X)$ to simulation results.

As a first example, we applied the pulling method to binary mixtures of benzene and pyridine, which are reasonably well described by regular solution theory, since the molecules are of similar size and shape, but interact differently because of the substantial dipole on pyridine.

We can observe how our simulations work qualitatively by comparing results for an equimolar mixture of labeled and unlabeled benzene in which the labeled benzene is pulled towards the center and unlabeled pushed away, with results for a equimolar mixture of benzene and pyridine, in which benzene is pulled inwards and pyridine pushed outwards. The concentration variation induced by the pushing and pulling is larger for the benzene-pyridine mixture than for the ideal mixture of labeled and unlabeled benzene. This result reflects the increased tendency of benzene and pyridine to demix because of the effective repulsive interactions between the two species.

Fitting the simulation results for $U_{ex}(X)$ for benzene-pyridine mixtures using TraPPE UA potentials to regular solution theory predictions gives χ per molecule equal to 0.763 ± 0.005. This value is consistent with χ determined using a recently developed "mutual ghosting" method.[15] In brief, the mutual ghosting method computes the mixing free energy by integrating the thermodynamic work to induce phase separation along a path on which

the attractions between two species are artificially weakened, and correcting for the interfacial tension of the resulting interface.

However, both values derived from UA simulations differ substantially from the experimental value of χ equal to 0.210 ± 0.004, determined from fitting regular solution theory to VLE data. We obtain much closer agreement with the pulling method using OPLS-AA all-atom potentials for benzene-pyridine mixtures, for which we obtain a χ value of 0.282 ± 0.002. This suggests that the TraPPE-UA potentials need to be tuned to better represent benzene-pyridine mixtures.

More broadly, these results highlight the importance of accurate potentials in simulations of mixtures, for which validation of the potentials against results for the pure fluids evidently does not always suffice. Evidently, where VLE or other data is available to obtain experimental χ parameters, the pulling method can be used to test and refine simulation potentials to better represent mixtures.

The pulling method is convenient and powerful, in that we can measure the exchange chemical potential over a range of species concentration from a single simulation. This is evidently more convenient than the mutual ghosting method, which requires a sequence of simulations at different interaction strengths, as well as an accurate measurement of the interfacial tension. Like mutual ghosting, the pulling method can be applied to chemically realistic systems as well as idealized bead-spring models, and does not require structural similarity between mixture components.

With some modifications, we can also employ the pulling method to investigate mixing free energies in polymer solutions and polymer-polymer blends. For such systems, Flory-Huggins theory rather than regular solution theory would be the simplest phenomenological model to use in fitting interaction parameters to simulation results. Gradient contributions to the local chemical potential may become important in applying the pulling method to oligomer blends, because the magnitude of ideal-mixing and relevant χ parameters both become smaller, so that gradient terms are no longer negligible by comparison.

Conflicts of interest

There are no conflicts to declare.

Acknowledgements

Financial support from the National Science Foundation under award DMR-1905632 is acknowledged.

Notes and references

1 M. Rubinstein and R. H. Colby, *Polymer Physics*, Oxford University Press, Oxford, 2003.

2 J. M. Stubbs and J. I. Siepmann, *The Journal of Physical Chemistry B*, 2002, **106**, 3968–3978.

3 J. J. de Pablo, M. Laso and U. W. Suter, *The Journal of Chemical Physics*, 1992, **96**, 6157–6162.

4 F. A. Escobedo and J. J. d. Pablo, *The Journal of Chemical Physics*, 1996, **105**, 4391–4394.

5 C. Perego, F. Giberti and M. Parrinello, *The European Physical Journal Special Topics*, 2016, **225**, 1621–1628.

6 J. G. Kirkwood and F. P. Buff, *The Journal of Chemical Physics*, 1951, **19**, 774–777.

7 P. Ganguly, D. Mukherji, C. Junghans and N. F. A. v. d. Vegt, *Journal of Chemical Theory and Computation*, 2012, **8**, 1802–1807.

8 F. Venetsanos, S. D. Anogiannakis and D. N. Theodorou, *Macromolecules*, 2022, **55**, 4852–4862.

9 P. C. Petris, S. D. Anogiannakis, P.-N. Tzounis and D. N. Theodorou, *The Journal of Physical Chemistry B*, 2019, **123**, 247–257.

10 M. Heidari, K. Kremer, R. Cortes-Huerto and R. Potestio, *Journal of Chemical Theory and Computation*, 2018, **14**, 3409–3417.

11 S. Shetty, M. M. Adams, E. D. Gomez and S. T. Milner, *Macromolecules*, 2020, **53**, 9386–9396.

12 S. Shetty, E. D. Gomez and S. T. Milner, *Macromolecules*, 2021, **54**, 10447–10455.

13 D. J. Kozuch, W. Zhang and S. T. Milner, *Polymers*, 2016, **8**, 241.

14 W. Zhang, E. D. Gomez and S. T. Milner, *Physical Review Letters*, 2017, **119**, 017801.

15 S. Shetty, P. Agarwala, E. D. Gomez and S. T. Milner, submitted for publication in Journal of Chemical Theory and Computation (2022).

16 W. Humphrey, A. Dalke and K. Schulten, *Journal of Molecular Graphics*, 1996, **14**, 33–38.

17 A. S. Mehrotra, S. Puri and D. V. Khakhar, *Physical Review E*, 2011, **83**, 061306.

18 P. Atkins and J. de Paula, *Atkins' Physical Chemistry (Eighth Edition)*, Oxford University Press, Oxford, 2006.

19 P. Garrett, J. Pollock and K. Morcom, *The Journal of Chemical Thermodynamics*, 1973, **5**, 569–575.

20 M. G. Martin and J. I. Siepmann, *The Journal of Physical Chemistry B*, 1998, **102**, 2569–2577.

21 M. G. Martin and J. I. Siepmann, *The Journal of Physical Chemistry B*, 1999, **103**, 4508–4517.

22 B. Chen, J. J. Potoff and J. I. Siepmann, *The Journal of Physical Chemistry B*, 2001, **105**, 3093–3104.

23 W. L. Jorgensen, *The Journal of Physical Chemistry*, 1986, **90**, 1276 – 1284.

24 W. L. Jorgensen, D. S. Maxwell and J. Tirado-Rives, *Journal of the American Chemical Society*, 1996, **118**, 11225–11236.

25 W. L. Jorgensen and J. Tirado-Rives, *Proceedings Of The National Academy Of Sciences*, 2005, **102**, 6665 – 6670.